

Microchip Yb:CaLnAlO₄ lasers with up to 91% slope efficiency

PAVEL LOIKO,^{1,2} JOSEP MARIA SERRES,¹ XAVIER MATEOS,^{1,3,*} XIAODONG XU,⁴ JUN XU,⁵ VENKATESAN JAMBUNATHAN,⁶ PETR NAVRATIL,⁶ ANTONIO LUCIANETTI,⁶ TOMAS MOCEK,⁶ XUZHAO ZHANG,¹ UWE GRIEBNER,³ VALENTIN PETROV,³ MAGDALENA AGUILÓ,¹ FRANCESC DÍAZ,¹ AND ARKADY MAJOR⁷

¹Física i Cristal·lografia de Materials i Nanomaterials (FiCMA-FiCNA)-EMaS, Dept. Química Física i Inòrganica, Universitat Rovira i Virgili (URV), Campus Sescelades, E-43007 Tarragona, Spain

²ITMO University, 49 Kronverkskiy pr., 197101 St. Petersburg, Russia

³Max Born Institute for Nonlinear Optics and Short Pulse Spectroscopy, Max-Born-Str. 2a, D-12489 Berlin, Germany

⁴Jiangsu Key Laboratory of Advanced Laser Materials and Devices, School of Physics and Electronic Engineering, Jiangsu Normal University, 221116 Xuzhou, China

⁵School of Physics Science and Engineering, Institute for Advanced Study, Tongji University, 200092 Shanghai, China

⁶HiLASE Centre, Institute of Physics CAS, Za Radnicí 828, 25241 Dolní Břežany, Czech Republic

⁷Department of Electrical and Computer Engineering, University of Manitoba, 75A Chancellors Circle, Winnipeg, MB, R3T 5V6, Canada

*Corresponding author: xavier.mateos@urv.cat, mateos@mbi-berlin.de

Received XX Month XXXX; revised XX Month, XXXX; accepted XX Month XXXX; posted XX Month XXXX (Doc. ID XXXXX); published XX Month XXXX

Multi watt continuous-wave operation of tetragonal rare-earth calcium aluminate Yb:CaLnAlO₄ (Ln = Gd, Y) crystals in plano-plano microchip laser was demonstrated with an almost quantum-defect-limited slope efficiency. Pumped at 978 nm by an InGaAs laser diode, a 3.4 mm-long 8 at.% Yb:CaGdAlO₄ laser generated 7.79 W at 1057–1065 nm with a slope efficiency of $\eta = 84\%$ (with respect to the absorbed pump power). Even higher $\eta = 91\%$ was achieved with a 2.5 mm-long 3 at.% Yb:CaYAlO₄ laser, from which 5.06 W were extracted at 1048–1056 nm. Both lasers produced linearly polarized output (σ -polarization) with an almost circular diffraction-limited beam ($M^2_{x,y} < 1.1$). The output performance of the developed lasers was modelled yielding an internal loss coefficient as low as 0.004–0.007 cm⁻¹. In addition, their spectroscopic properties were revisited.

OCIS codes: (140.3380) Laser materials; (300.0300) Spectroscopy; (140.3480) Lasers, diode-pumped.

<http://dx.doi.org/10.1364/OL.99.099999>

The development of compact lasers comprising a gain material and (optionally) a saturable absorber placed between two plane cavity mirrors (in the so-called microchip laser geometry) is of practical interest since such devices offer numerous advantages [1]. In the continuous-wave (CW) operation mode they benefit

from low-loss, robustness and insensitivity to misalignment, as well as good mode-matching provided by the induced thermal lens [2]. As a consequence, high laser efficiency is possible. In the passively Q-switched (PQS) regime, they generate very short pulses (down to sub-ns in duration) due to the reduced cavity roundtrip time [3–5]. The laser material intended for use in microchip lasers should combine certain spectroscopic and thermal / thermo-optic properties. The former group includes high doping levels, high transition cross-sections leading to a high pump efficiency and low laser threshold, as well as relatively long upper laser lifetime leading to pulse energy scaling capabilities for the PQS regime [4,5]. The latter group includes high thermal conductivity and positive thermal lensing [2].

The Ytterbium (Yb³⁺) ion is well-known for its laser emission at $\sim 1 \mu\text{m}$ related to the $^2F_{5/2} \rightarrow ^2F_{7/2}$ transition. Its simple energy level scheme disables parasitic excited-state absorption and upconversion processes, leading to low heat loading. Yb³⁺-doped crystals can easily be pumped by commercially available high-power InGaAs laser diodes. To date, there is a variety of laser hosts studied for Yb³⁺ doping [6]. Over the past decade, Yb³⁺-lasers have become the choice for high power operation. At the same time, only few materials were studied in highly-efficient power-scalable compact (incl. microchip-type) lasers [7–11].

One type of crystals which is known to be very suitable for power-scalable CW and especially mode-locked (ML) Yb lasers are the tetragonal rare-earth calcium aluminates Yb:CaLnAlO₄ (where Ln = Gd or Y [12,13]), denoted shortly as CALGO or CALYO,

respectively. These crystals exhibit local disorder [14] and when doped with Yb^{3+} ions, this is manifested in broad and smooth spectral bands. Doping concentrations as high 15 at.% are feasible for Yb:CaLnAlO_4 crystals. Their thermal conductivity is rather high (3-6 W/mK) for disordered crystals and shows weak dependence on the Yb^{3+} doping level [15]. In addition, positive thermal lens was reported for various Yb:CaLGO crystal orientations [16].

The CW and ML performance of Yb:CaLnAlO_4 crystals has been extensively studied in the last decade. Sub-50 fs pulses were achieved using semiconductor saturable absorbers (SESAMs) and Kerr-lens mode-locking [17-19]. High-power bulk and thin-disk Yb:CaLGO lasers were also reported [10,16,20]. However, to date, Yb:CaLnAlO_4 crystals have not been used in microchip lasers. In the present work, we report on various Yb:CaLnAlO_4 microchip lasers demonstrating almost quantum-defect-limited laser slope efficiency and multi-watt CW output power.

CaLnAlO_4 crystals belong to the family of crystals with general formula ABC_4 where $A = \text{Ca}$ or Sr , $B = \text{Y}$ or rare-earth ion, $C = \text{Al}$ or Ga . They are tetragonal (sp. gr. $I4/mmm$, D_{17h}^{14}), with lattice parameters $a = 3.663 \text{ \AA}$ and $c = 12.010 \text{ \AA}$ for CALGO and $a = 3.645 \text{ \AA}$ and $c = 11.874 \text{ \AA}$ for CALYO. Yb^{3+} substitutes the passive Ln^{3+} in a site with a point symmetry C_{4v} and IX-fold O^{2-} -coordination which otherwise is statistically occupied by Ca^{2+} and Ln^{3+} ions due to the closeness of their ionic radii. In doped crystals, the local disorder originates from the second coordination sphere of the Yb^{3+} cations by the Ca^{2+} and Ln^{3+} ions (due to the charge difference of these ions and the different cation-cation distances) [14]. The ionic radii of IX-fold coordinated Y^{3+} (1.075 \AA) and Gd^{3+} (1.107 \AA) are slightly larger than that of Yb^{3+} (1.042 \AA) and therefore relatively high Yb^{3+} doping levels are possible.

The CaLnAlO_4 crystals are optically uniaxial, the optic axis is parallel to the crystallographic c -axis. Thus, there are two principal refractive indices, n_o and n_e , see Table 1 [21], and two principal polarizations for doped CaLnAlO_4 crystals, $E \parallel c$ (π) and $E \perp c$ (σ).

Table 1 Optical and Thermo-Optical Parameters of CaLnAlO_4 crystals at $\sim 1 \mu\text{m}$

Crystal	$n_{o(e)}$	$dn_{o(e)}/dT$, 10^{-6} K^{-1}	M (α -cut, σ)*, m^{-1}/W
CALGO	1.918 (o), 1.941 (e)	-7.6 (o), -8.6 (e)	0.38
CALYO	1.886 (o), 1.909 (e)	-7.8 (o), -8.7 (e)	0.36

*Diode-pumping: $\lambda_p = 978 \text{ nm}$, $w_p = 100 \mu\text{m}$.

In the present work, 8 at.% Yb:CaLGO and 3 at.% Yb:CaLYO crystals were grown by the Czochralski method and annealed in a reducing atmosphere to eliminate the color centers. The obtained crystals were transparent and colorless. The laser elements were oriented for light propagation along the α -axis (α -cut). Their thickness was 3.4 mm (Yb:CaLGO) or 2.5 mm (Yb:CaLYO), and the aperture was $3 \times 3 \text{ mm}^2$. Both input and output faces of the samples were polished to laser grade quality and remained uncoated.

At first, we revisited the absorption, σ_{abs} , and stimulated-emission (SE), σ_{SE} , cross-sections for the Yb:CaLnAlO_4 crystals. This was needed because of the strong discrepancy found in the literature [12,13,22,23], partially due to the lack of refractive index data, which was reported only very recently [21]. In the present work, σ_{SE} was calculated with the modified reciprocity method

[24] using the following Yb^{3+} lifetimes: $\tau_{\text{Yb}} = 420$ and $426 \mu\text{s}$ for Yb:CaLGO and Yb:CaLYO , respectively [13]. The results are shown in Fig. 1. The values, if calculated by the standard reciprocity method, would correspond to a ratio of the partition functions for the ground- and excited-state $Z_g/Z_e \sim 1.24$ which is very close to the value obtained from the published Stark splitting of the Yb^{3+} multiplets in CALYO (1.195) [22]. As already mentioned, the disordered structure of Yb:CaLnAlO_4 leads to inhomogeneous broadening of the absorption and emission bands. The maximum σ_{abs} for the π -polarization (corresponding to the zero-phonon line (ZPL), in both crystals at $\lambda_0 = 979.5 \text{ nm}$, or $E_0 = 10209 \text{ cm}^{-1}$) is $2.6 \times 10^{-20} \text{ cm}^2$ for Yb:CaLGO and $3.5 \times 10^{-20} \text{ cm}^2$ for Yb:CaLYO . The corresponding full width at half maximum (FWHM) of the absorption band is ~ 6 and 10 nm , respectively. For the σ -polarization, σ_{abs} at λ_0 is roughly 2 times lower, $\sim 1.4 \times 10^{-20}$ and $1.5 \times 10^{-20} \text{ cm}^2$ for Yb:CaLGO and Yb:CaLYO , respectively. Consequently, Yb:CaLYO provides higher σ_{abs} and broader ZPL absorption peak. As for the SE cross-sections, since Yb^{3+} ions represent a quasi-three-level laser scheme, laser operation is expected at the long-wavelength part of the σ_{SE} spectra. In this spectral range for both crystals σ_{SE} is higher for the σ -polarization: $0.65 \times 10^{-20} \text{ cm}^2$ at $\sim 1035 \text{ nm}$ for Yb:CaLGO and $0.58 \times 10^{-20} \text{ cm}^2$ at $\sim 1046 \text{ nm}$ for Yb:CaLYO . Consequently, Yb:CaLGO is more attractive because of slightly higher σ_{SE} .

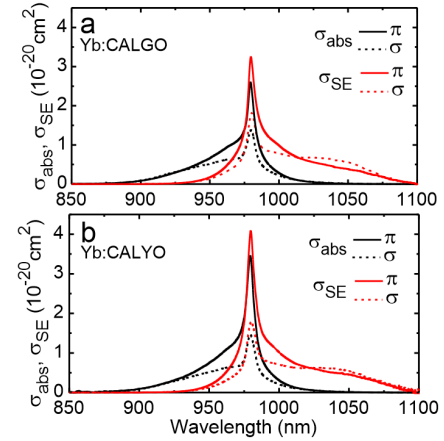


Fig. 1. Absorption, σ_{abs} , and stimulated-emission, σ_{SE} , cross-sections of Yb^{3+} :CALGO (a) and Yb^{3+} :CALYO (b) for the π and σ light polarizations.

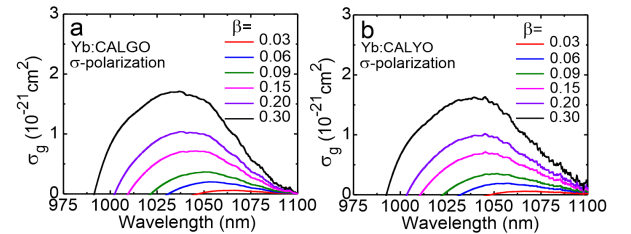


Fig. 2. Gain cross-sections, $\sigma_g = \beta\sigma_{\text{SE}} - (1 - \beta)\sigma_{\text{abs}}$, for Yb^{3+} :CALGO (a) and Yb^{3+} :CALYO (b) for the σ -polarization and different inversion ratios β .

The gain cross-section, $\sigma_g = \beta\sigma_{SE} - (1 - \beta)\sigma_{abs}$, spectra of Yb^{3+} in CaLnAlO_4 crystals are shown in Fig. 2 (for the σ -polarization). Here, β is the inversion ratio, $\beta = N_2(2F_{5/2})/N_{\text{Yb}}$, where N_{Yb} is the actual doping concentration.

The laser performance of Yb:CaLnAlO_4 crystals was studied in a compact plano-plano cavity. Laser operation with such a cavity is possible only when a positive thermal lens is provided by the crystal. However, it is known that the thermo-optic coefficients of both CaLnAlO_4 crystals are negative [15] as shown in Table 1. This is overcome by their large and positive thermal expansion leading to a nearly-athermal behavior [15,25]. In the present work, we determined the sensitivity factors of the thermal lens $M = dD/dP_{abs}$ (D is the optical (refractive) power of the thermal lens, P_{abs} is the absorbed pump power, see details in [7]) for the α -cut Yb:CaLnAlO_4 and Yb:CaLYO and σ -polarization as $0.38 \text{ m}^{-1}/\text{W}$ and $0.36 \text{ m}^{-1}/\text{W}$, respectively (diode-pumping, $\lambda_p = 978 \text{ nm}$, pump spot radius $w_p = 100 \mu\text{m}$). Thus, microchip laser operation is possible with both Yb:CaLnAlO_4 crystals.

The designed laser cavity, see the scheme in [7], consisted of a flat pump mirror (PM) that was antireflection (AR) coated for 900–1000 nm and highly-reflective (HR) coated for 1020–1200 nm, and a flat output coupler (OC) with transmission $T_{OC} = 1\%$, 2.5% , 5% or 10% at the laser wavelength. Both PM and OC were located as close as possible to the crystal faces, so that the geometrical cavity length was equal to the crystal length (3.4 or 2.5 mm). The laser crystals were pumped through the PM by a fiber-coupled InGaAs laser diode (fiber core diameter: $200 \mu\text{m}$, N.A. = 0.22) emitting up to 20 W at $\sim 978 \text{ nm}$ (emission bandwidth: 2 nm). The diode emission wavelength was stabilized by water-cooling. A lens assembly with an imaging ratio of 1:1 and a focal length of 30 mm provided a pump spot radius of $w_p = 100 \mu\text{m}$ in the crystal. The confocal parameter for the pump beam $2Z_R$ was 1.75 mm ($M^2 \sim 70$). The pump radiation was unpolarized. The crystals were pumped in a double pass configuration due to the partial reflection ($\sim 90\%$) of the OC at the pump wavelength. The total pump absorption under lasing conditions was determined from the pump-transmission experiment and rate-equation modelling accounting for the ground-state bleaching [26] as 73% (for Yb:CaLnAlO_4) and 47% (for Yb:CaLYO). The radius of the laser mode in the crystal was calculated with the ABCD-modelling using the determined parameters of the thermal lens [2] as $w_L = 100 \pm 10 \mu\text{m}$.

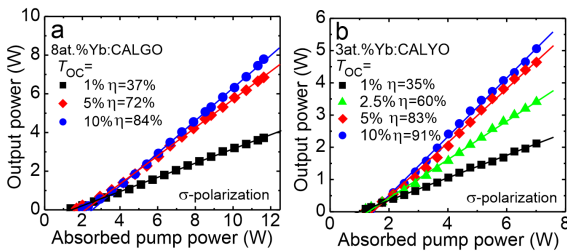


Fig. 3. Input-output dependences for Yb:CaLnAlO_4 (a) and Yb:CaLYO (b) microchip lasers ($w_p = 100 \mu\text{m}$), η – slope efficiency.

Laser operation in the plano-plano cavity was achieved with both Yb:CaLnAlO_4 crystals. The laser output was linearly polarized (σ) and no polarization switching was observed. The input-output

dependences are shown in Fig. 3. For Yb:CaLnAlO_4 , the maximum output power reached 7.79 W at 1057–1065 nm with a slope efficiency η of 84% (versus P_{abs}) for $T_{OC} = 10\%$. The laser threshold was at $P_{th} = 2.0 \text{ W}$ and the optical-to-optical efficiency (versus incident pump power) reached $\eta_{opt} = 49\%$. For $T_{OC} = 5\%$ and 1% , the slope efficiency was lower, $\eta = 72\%$ and 37% , respectively. For Yb:CaLYO , the maximum laser output reached 5.06 W at 1048–1056 nm corresponding to a record high $\eta = 91\%$ connected with a lower laser threshold ($P_{th} = 1.4 \text{ W}$) and $\eta_{opt} = 32\%$.

Neither roll-over of the output power nor the stress fracture were observed for both studied Yb:CaLnAlO_4 microchip lasers (at least up to $P_{abs} = 11.6 \text{ W}$), thanks to the relatively high thermal conductivity of these compounds ($\kappa \sim 5.6 \text{ W/mK}$ for 8 at.% Yb:CaLnAlO_4) and the low anisotropy of their thermal expansion ($\alpha_c/\alpha_a = 1.4\dots 1.6$) [15].

The laser emission spectra of the Yb:CaLnAlO_4 microchip lasers are shown in Fig. 4. The spectra exhibit a multi-peak behavior due to the broad gain spectra of the Yb^{3+} ion (Fig. 2) and etalon effects due to the small separations between the PM, laser crystal and OC. For Yb:CaLnAlO_4 , at low $T_{OC} = 1\%$, the laser emitted at 1069–1080 nm and for the higher T_{OC} , the spectra shifted to shorter wavelengths, 1057–1068 nm. For Yb:CaLYO , the emission spectra were weakly dependent on T_{OC} and emission in the 1048–1064 nm range was observed. Such spectral behavior agrees with the σ_g spectra (for small $\beta < 0.1$), see Fig. 2 and is common in Yb^{3+} gain media [27].

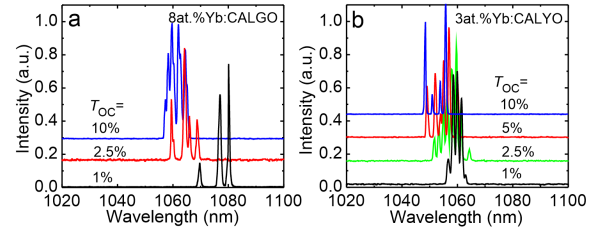


Fig. 4. Laser emission spectra for the Yb:CaLnAlO_4 (a) and Yb:CaLYO (b) microchip lasers, measured at maximum P_{abs} according to Fig. 3.

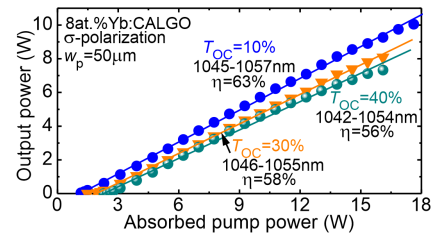


Fig. 5. Input-output characteristics of the Yb:CaLnAlO_4 laser pumped by a VBG-stabilized diode at 981 nm ($w_p = 50 \mu\text{m}$), η – slope efficiency.

The output characteristics of the Yb:CaLnAlO_4 microchip lasers were simulated with a model of a quasi-three-level laser [26] using the revisited spectroscopic parameters, Fig. 1. Based on this model, we estimated the internal losses in the 8 at.% Yb:CaLnAlO_4 and 3 at.% Yb:CaLYO crystals to be as low as $\delta = 0.0067 \pm 0.0008 \text{ cm}^{-1}$ and $0.0042 \pm 0.0006 \text{ cm}^{-1}$, respectively. A lower η for the 8 at.% Yb doped crystal is due to the higher losses and partially due to the

stronger cooperative processes for the Yb^{3+} - Yb^{3+} ion pairs. It is worth noting that the corresponding blue emission was very weak for both $\text{Yb}:\text{CaLnAlO}_4$ crystals.

In Fig. 3, power scaling of the $\text{Yb}:\text{CaLnAlO}_4$ microchip lasers was limited by the available pump power. Thus, we have employed a different pump source, namely a VBG-stabilized InGaAs diode emitting up to 27 W at 981 nm (fiber core diameter: 105 μm , N.A.: 0.22) which ensures higher total pump absorption ($\sim 80\%$ for $\text{Yb}:\text{CALGO}$) with a smaller pump spot radius of $w_p = 50 \mu\text{m}$. The output characteristics of the $\text{Yb}:\text{CALGO}$ microchip laser pumped by the unpolarized output of the VBG-stabilized diode are shown in Fig. 5. The maximum output power reached 10.05 W at 1045-1057 nm with $\eta = 63\%$ and $\eta_{\text{opt}} = 46\%$. The laser threshold was at $P_{\text{th}} = 1.05 \text{ W}$. The lower laser efficiency with respect to Fig. 3(a) can be explained by the worse mode-matching due to the stronger thermal lens (as $M \sim 1/w_p^2$) and stronger divergence of the pump beam ($2z_R = 0.83 \text{ mm}$). Thus, larger w_p is desirable for high laser efficiency in the $\text{Yb}:\text{CALGO}$ microchip lasers. Multi-watt operation of this laser with high output coupling is a promising indication for further development of PQS oscillators where high T_{oc} is needed to reduce the damage probability of optical surfaces.

All the studied $\text{Yb}:\text{CaLnAlO}_4$ microchip lasers generated a nearly circular output beam, see Fig. 6. The circular beam profile indicates a very low astigmatism of the thermal lens (estimated in the present paper to be $S/M < 10\%$ for both crystals).

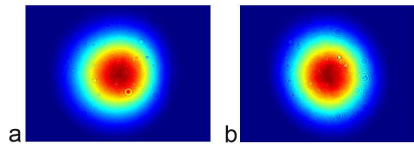


Fig. 6. Spatial profiles of the $\text{Yb}:\text{CALGO}$ (a) and $\text{Yb}:\text{CALYO}$ (b) microchip lasers, $T_{\text{oc}} = 10\%$, $P_{\text{abs}} = 11.6 \text{ W}$ (a) or 7.0 W (b).

In conclusion, the ytterbium-doped rare-earth calcium aluminates, $\text{Yb}:\text{CaLnAlO}_4$, are very promising for microchip lasers as they provide high Yb^{3+} doping levels, broad spectral bands, weak and positive thermal lensing allowing for good mode-matching for a broad range of pump powers, high thermal conductivity and low internal losses resulting in nearly linear output dependence and very high laser slope efficiency. We presented the first $\text{Yb}:\text{CaLnAlO}_4$ plano-plano microchip lasers which generated multi-watt CW output with record and almost quantum-defect-limited laser slope efficiencies of 84% and 91%, respectively, when pumped with a fiber-coupled InGaAs laser diode at $\sim 978 \text{ nm}$. For an α -cut 8 at% $\text{Yb}:\text{CALGO}$, the output power was scaled up to $\sim 7.8 \text{ W}$ (with $\eta = 84\%$) or even up to $\sim 10 \text{ W}$ (with lower $\eta = 63\%$) at the emission wavelength of $\sim 1050 \text{ nm}$.

The $\text{Yb}:\text{CaLnAlO}_4$ crystals are promising for PQS microchip lasers potentially generating sub-ns pulses. Indeed, the lifetime of the Yb^{3+} ion in CALGO and CALYO is almost two times longer as compared with the $\text{Yb}:\text{KLu}(\text{WO}_4)_2$ successfully used in this type of lasers [4]. An additional benefit of $\text{Yb}:\text{CaLnAlO}_4$ as compared with $\text{Yb}:\text{KLu}(\text{WO}_4)_2$ is a much weaker thermal lens leading to a larger size of the laser mode and, consequently, lower probability of laser-induced damage. By inserting a Cr:YAG saturable absorber

into such microchip lasers, we expect to generate short pulses with energies of hundreds of μJ and peak powers exceeding 100 kW.

Funding. Spanish Government (MAT2016-75716-C2-1-R, (AEI/FEDER/UE), MAT2013-47395-C4-4-R, TEC 2014-55948-R); Generalitat de Catalunya (2014SGR1358). Czech Republic and the Ministry of Education, Youth and Sports (Programs NPU I – project no. LO1602, and Large Research Infrastructure – project no. LM2015086); NSERC Discovery.

Acknowledgment. F.D. acknowledges additional support through the ICREA academia award 2010ICREA-02 for excellence in research. X.M. acknowledges support from the European Union's Horizon 2020 research and innovation programme under the Marie Skłodowska-Curie grant agreement No 657630. P.L. acknowledges financial support from the Government of the Russian Federation (Grant 074-U01) through ITMO Post-Doctoral Fellowship scheme.

References

- J. J. Zayhowski, *Opt. Mater.* **11**, 255 (1999).
- J. M. Serres, X. Mateos, P. Loiko, K. Yumashev, N. Kuleshov, V. Petrov, U. Griebner, M. Aguiló, and F. Díaz, *Opt. Lett.* **39**, 4247 (2014).
- J. J. Zayhowski and C. Dill, *Opt. Lett.* **19**, 1427 (1994).
- P. Loiko, J. M. Serres, X. Mateos, K. Yumashev, A. Yasukevich, V. Petrov, U. Griebner, M. Aguiló, and F. Díaz, *Opt. Lett.* **41**, 2620 (2016).
- J. Dong, K. Ueda, A. Shirakawa, H. Yagi, T. Yanagitani, and A. A. Kaminskii, *Opt. Express* **15**, 14516 (2007).
- W. F. Krupke, *IEEE J. Sel. Top. Quantum Electron.* **6**, 1287 (2000).
- P. Loiko, J. M. Serres, X. Mateos, H. Yu, H. Zhang, J. Liu, K. Yumashev, U. Griebner, V. Petrov, M. Aguiló, and F. Díaz, *IEEE Photonics J.* **8**, 1501312 (2016).
- T. Dascalu, T. Taira, and N. Pavel, *Opt. Lett.* **27**, 1791-1793 (2002).
- J. Dong, K. Ueda, H. Yagi, A. A. Kaminskii, and Z. Cai, *Laser Phys. Lett.* **6**, 282-289 (2009).
- W. D. Tan, D. Y. Tang, X. D. Xu, D. Z. Li, J. Zhang, C. W. Xu, Z. H. Cong, and J. Xu, *Laser Phys. Lett.* **8**, 193-196 (2011).
- S. Wang, K. Wu, Y. Wang, H. Yu, H. Zhang, X. Tian, Q. Dai, and J. Liu, *Opt. Express* **21**, 16305-16310 (2013).
- J. Petit, P. Goldner, and B. Viana, *Opt. Lett.* **30**, 1345 (2005).
- D. Li, X. Xu, Y. Cheng, S. Cheng, D. Zhou, F. Wu, C. Xia, J. Xu, and J. Zhang, *J. Cryst. Growth* **312**, 2117 (2010).
- P. O. Petit, J. Petit, Ph. Goldner, and B. Viana, *Opt. Mater.* **30**, 1093 (2008).
- P. Loiko, F. Druon, P. Georges, B. Viana, and K. Yumashev, *Opt. Mater. Express* **4**, 2241 (2014).
- F. Druon, M. Olivier, A. Jaffrès, P. Loiseau, N. Aubry, J. Didierjean, F. Balembois, B. Viana, and P. Georges, *Opt. Lett.* **38**, 4138 (2013).
- Y. Zaouter, J. Didierjean, F. Balembois, G. Lucas Leclin, F. Druon, P. Georges, J. Petit, P. Goldner, and B. Viana, *Opt. Lett.* **31**, 119 (2006).
- P. Sévillano, P. Georges, F. Druon, D. Descamps, and E. Cormier, *Opt. Lett.* **39**, 6001 (2014).
- S. Manjooan and A. Major, in *Conference on Lasers and Electro-Optics (Optical Society of America, 2016)*, P. JTu5A.82.
- K. Beil, B. Deppe, and C. Kränkel, *Opt. Lett.* **38**, 1966 (2013).
- P. Becker, L. Bohatý, C. Liebald, M. Peltz, S. Vernay, D. Rytz, P. Loiko, J. M. Serres, X. Mateos, K. Yumashev, Y. Wang, V. Petrov, and U. Griebner, in *7th EPS-QEOD Europhoton Conference, Vienna, Austria, August, 21–26, 2016*, P. PO-3.13 (2016).
- J. A. Hutchinson, H. R. Verdun, B. H. T. Chai, B. Zandi, and L. D. Merkle, *Opt. Mater.* **3**, 287 (1994).

23. A. Rudenkov, V. Kisel, A. Yasukevich, K. Hovhannesian, A. Petrosyan, and N. Kuleshov, *Opt. Lett.* **41**, 2249 (2016).
24. A. S. Yasyukevich, V. G. Shcherbitskii, V. E. Kisel, A. V. Mandrik, and N. V. Kuleshov, *J. Appl. Spectr.* **71**, 202 (2004).
25. J. Petit, P. Goldner, B. Viana, J. Didierjean, F. Balembois, F. P. Druon, and P. Georges, in *Advanced Solid-State Photonics, Technical Digest (Optical Society of America, 2006)*, P. WD1.
26. R. Lan, P. Loiko, X. Mateos, Y. Wang, J. Li, Y. Pan, S. Y. Choi, M. H. Kim, F. Rotermund, A. Yasukevich, K. Yumashev, U. Griebner, and V. Petrov, *Appl. Opt.* **55**, 4877 (2016).
27. H. Zhao and A. Major, *Opt. Express* **22**, 26651 (2014).

References

1. J. J. Zayhowski, "Microchip lasers," *Opt. Mater.* **11**(2-3), 255-267 (1999).
2. J. M. Serres, X. Mateos, P. Loiko, K. Yumashev, N. Kuleshov, V. Petrov, U. Griebner, M. Aguiló, and F. Díaz, "Diode-pumped microchip Tm:KLu(WO₄)₂ laser with more than 3 W of output power," *Opt. Lett.* **39**(14), 4247-4250 (2014).
3. J. J. Zayhowski and C. Dill, "Diode-pumped passively Q-switched picosecond microchip lasers," *Opt. Lett.* **19**(18), 1427-1429 (1994).
4. P. Loiko, J. M. Serres, X. Mateos, K. Yumashev, A. Yasukevich, V. Petrov, U. Griebner, M. Aguiló, and F. Díaz, "Sub-nanosecond Yb:KLu(WO₄)₂ microchip laser," *Opt. Lett.* **41**(11), 2620-2623 (2016).
5. J. Dong, K. Ueda, A. Shirakawa, H. Yagi, T. Yanagitani, and A. A. Kaminskii, "Composite Yb:YAG/Cr⁴⁺:YAG ceramics picosecond microchip lasers," *Opt. Express* **15**(22), 14516-14523 (2007).
6. W. F. Krupke, "Ytterbium solid-state lasers. The first decade," *IEEE J. Sel. Top. Quantum Electron.* **6**(6), 1287-1296 (2000).
7. P. Loiko, J. M. Serres, X. Mateos, H. Yu, H. Zhang, J. Liu, K. Yumashev, U. Griebner, V. Petrov, M. Aguiló, and F. Díaz, "Thermal lensing and multi-watt microchip laser operation of Yb:YCOB crystals," *IEEE Photonics J.* **8**(3), 1501312-1-12 (2016).
8. T. Dascalu, T. Taira, and N. Pavel, "100-W quasi-continuous-wave diode radially pumped microchip composite Yb:YAG laser," *Opt. Lett.* **27**(20), 1791-1793 (2002).
9. J. Dong, K. Ueda, H. Yagi, A. A. Kaminskii, and Z. Cai, "Comparative study the effect of Yb concentrations on laser characteristics of Yb:YAG ceramics and crystals," *Laser Phys. Lett.* **6**(4), 282-289 (2009).
10. W. D. Tan, D. Y. Tang, X. D. Xu, D. Z. Li, J. Zhang, C. W. Xu, Z. H. Cong, and J. Xu, "Room temperature diode-pumped Yb:CaYAlO₄ laser with near quantum limit slope efficiency," *Laser Phys. Lett.* **8**(3), 193-196 (2011).
11. S. Wang, K. Wu, Y. Wang, H. Yu, H. Zhang, X. Tian, Q. Dai, and J. Liu, "Spectral and lasing investigations of Yb:YSGG crystal," *Opt. Express* **21**(14), 16305-16310 (2013).
12. J. Petit, P. Goldner, and B. Viana, "Laser emission with low quantum defect in Yb:CaGdAlO₄," *Opt. Lett.* **30**(11), 1345-1347 (2005).
13. D. Li, X. Xu, Y. Cheng, S. Cheng, D. Zhou, F. Wu, C. Xia, J. Xu, and J. Zhang, "Crystal growth and spectroscopic properties of Yb:CaYAlO₄ single crystal," *J. Cryst. Growth* **312**(14), 2117-2121 (2010).
14. P. O. Petit, J. Petit, Ph. Goldner, and B. Viana, "Inhomogeneous broadening of optical transitions in Yb:CaYAlO₄," *Opt. Mater.* **30**(7), 1093-1097 (2008).
15. P. Loiko, F. Druon, P. Georges, B. Viana, and K. Yumashev, "Thermo-optic characterization of Yb:CaGdAlO₄ laser crystal," *Opt. Mater. Express* **4**(11), 2241-2249 (2014).
16. F. Druon, M. Olivier, A. Jaffrès, P. Loiseau, N. Aubry, J. DidierJean, F. Balembois, B. Viana, and P. Georges, "Magic mode switching in Yb:CaGdAlO₄ laser under high pump power," *Opt. Lett.* **38**(20), 4138-4141 (2013).
17. Y. Zaouter, J. Didierjean, F. Balembois, G. Lucas Leclin, F. Druon, P. Georges, J. Petit, P. Goldner, and B. Viana, "47-fs diode-pumped Yb³⁺:CaGdAlO₄ laser," *Opt. Lett.* **31**(1), 119-121 (2006).
18. P. Sévillano, P. Georges, F. Druon, D. Descamps, and E. Cormier, "32-fs Kerr-lens mode-locked Yb:CaGdAlO₄ oscillator optically pumped by a bright fiber laser," *Opt. Lett.* **39**(20), 6001-6004 (2014).
19. S. Manjorán and A. Major, "Generation of sub-50 fs pulses with >1.5 MW of peak power from a diode-pumped Yb:CALGO laser oscillator," in *Conference on Lasers and Electro-Optics (Optical Society of America, 2016)*, P. JTu5A.82.
20. K. Beil, B. Deppe, and C. Kränkel, "Yb:CaGdAlO₄ thin-disk laser with 70% slope efficiency and 90 nm wavelength tuning range," *Opt. Lett.* **38**(11), 1966-1968 (2013).
21. P. Becker, L. Bohatý, C. Liebald, M. Peltz, S. Vernay, D. Rytz, P. Loiko, J. M. Serres, X. Mateos, K. Yumashev, Y. Wang, V. Petrov, and U. Griebner, "Sellmeier equations for CaGdAlO₄ and CaYAlO₄ laser host crystals," in *7th EPS-QEOD Europhoton Conference, Vienna, Austria, August, 21-26, 2016*, P. PO-3.13 (2016).
22. J. A. Hutchinson, H. R. Verdun, B. H. T. Chai, B. Zandi, and L. D. Merkle, "Spectroscopic evaluation of CaYAlO₄ doped with trivalent Er, Tm, Yb and Ho for eyesafe laser applications," *Opt. Mater.* **3**(4), 287-306 (1994).
23. A. Rudenkov, V. Kisel, A. Yasukevich, K. Hovhannesyan, A. Petrosyan, and N. Kuleshov, "Yb³⁺:CaYAlO₄-based chirped pulse regenerative amplifier," *Opt. Lett.* **41**(10), 2249-2252 (2016).
24. A. S. Yasyukevich, V. G. Shcherbitskii, V. E. Kisel, A. V. Mandrik, and N. V. Kuleshov, "Integral method of reciprocity in the spectroscopy of laser crystals with impurity centers," *J. Appl. Spectr.* **71**(2), 202-208 (2004).
25. J. Petit, P. Goldner, B. Viana, J. Didierjean, F. Balembois, F. P. Druon, and P. Georges, "Quest of athermal solid-state laser: Case of Yb:CaGdAlO₄," in *Advanced Solid-State Photonics, Technical Digest (Optical Society of America, 2006)*, P. WD1.
26. R. Lan, P. Loiko, X. Mateos, Y. Wang, J. Li, Y. Pan, S. Y. Choi, M. H. Kim, F. Rotermund, A. Yasukevich, K. Yumashev, U. Griebner, and V. Petrov, "Passive Q-switching of microchip lasers based on Ho:YAG ceramic," *Appl. Opt.* **55**(18), 4877-4887 (2016).
27. H. Zhao and A. Major, "Dynamic characterization of intracavity losses in broadband quasi-three-level lasers," *Opt. Express* **22**, 26651-26658 (2014).